

# 1 Enhanced Bioremediation of Zinc and Cadmium from Oil-Contaminated 2 Sites Using Biochar-Amended Fungal Systems Involving *Aspergillus niveus* 3 and *Alternaria chlamydosporigena*.

Najwa Majrashi and Fuad Ameen\*

7 \*correspondence to: fuadameen@ksu.edu.sa

## 8 Abstract

9 Bioremediation of oil-contaminated sites, common in oil-producing regions, requires novel  
10 solutions, such as the one suggested here: combining fungal and biochar treatments. Fungal  
11 strains were isolated from metal and oil-polluted soils and evaluated for their resistance to zinc  
12 (Zn) and cadmium (Cd). Two strains, *Aspergillus niveus* (GenBank accession: PQ463633) and  
13 *Alternaria chlamydosporigena* (PQ463634), exhibited exceptional growth under metal stress,  
14 demonstrating considerable metal resistance. These strains were chosen for further  
15 bioremediation experiments. A substantial decrease of Zn and Cd concentrations was observed  
16 after fungal incubation. The incorporation of biochar significantly improved the effectiveness  
17 of the heavy metal removal, indicating a synergistic interaction between fungal biosorption and  
18 biochar-facilitated immobilization. Fourier-transform infrared (FTIR) spectroscopy  
19 demonstrated notable morphological and biochemical changes in the fungal biomass following  
20 exposure to Zn and Cd, signifying active metal-binding interactions and uptake processes. The  
21 equilibrium behavior of metal uptake was demonstrated with three isotherm models. The  
22 Langmuir model showed the greatest fit ( $R^2 > 0.98$ ), followed by the Freundlich model ( $R^2 =$   
23 0.92-0.95) and the Temkin model ( $R^2 = 0.85-0.89$ ). A homogenous, monolayer-driven  
24 biosorption of the metals is supported by the best fit of the Langmuir isotherm. Kinetic models  
25 were utilized to examine the rate and mechanism of the biosorption process. A high correlation  
26 coefficient ( $R^2 = 0.98$ ) for the pseudo-second-order model suggests that chemisorption is the  
27 primary mechanism for the uptake of Zn and Cd by biochar and fungi. It is concluded that the  
28 combination of biochar and the fungi *A. niveus* and *A. chlamydosporigena* offers an economical  
29 and environmentally sustainable remediation technique for soils contaminated with oil and  
30 heavy metals. The discovery is significantly advancing the creation of sustainable  
31 biotechnological approaches for environmental restoration in oil-contaminated material,  
32 providing a feasible alternative to traditional physicochemical procedures.

33 **Keywords:** Biochar; Bioremediation; Fungi; Heavy metal; Soil petroleum.

35 **1. Introduction**

36 Soil polluted by petroleum hydrocarbons and heavy metals is a global environmental issue.  
37 Over five million polluted sites covering ca. 500 million hectares were reported globally (Falih  
38 *et al.*, 2024; Hou *et al.*, 2025). The financial impact of this contamination surpasses US\$10  
39 billion each year, with considerable consequences for ecosystems and human health.  
40 Petroleum-derived pollutants are of particular concern because they can migrate into aquatic  
41 systems and groundwater, jeopardizing the unsaturated zone and drinking water supplies.  
42 Petrogenic heavy metals, such as Pb, Zn, Ni, Mn, Cr, Fe, and Cd, exhibit enduring  
43 environmental deposition, particularly in oil-producing areas (Nna, Orie en Kalu, 2024).

44 The region around the Arabian Gulf serves as a case study, where sixty years of oil extraction  
45 and conflict-induced spills have resulted in severe metal contamination of coastal sediments  
46 and terrestrial ecosystems. Due to the contamination, large areas of land are unsuitable for  
47 agriculture, necessitating immediate remediation actions. Traditional methods for cleaning up  
48 the contamination, such as soil vapor extraction and thermal remediation, are too expensive  
49 and harmful to the environment, while bioremediation offers a more sustainable and cost-  
50 effective solution (Liu *et al.*, 2024).

51 Bioremediation utilizing fungi has proven to be promising. Certain fungi such as *Aspergillus*,  
52 *Penicillium*, and *Fusarium* remove efficiently metals from the environment because of their  
53 ability to bind metals to their cell walls and store metals inside their cells (Dinakarkumar *et al.*,  
54 2024). When combined with biochar, a type of carbon produced by heating organic material,  
55 fungi can be even more efficient (W. Wang *et al.*, 2024; Xia *et al.*, 2025). In bioremediation *in*  
56 *situ*, it is important to use local microbial isolates. In the Arabian Peninsula, information on  
57 such indigenous isolates is scarce. A recent review lists bacteria and fungi isolated from  
58 petroleum refinery effluents in India, Nigeria, Malaysia, South Africa, and Iraq. In Iraq, the  
59 fungal species were *Penicillium* sp., *Aspergillus fumigatus*, *Aspergillus niger*, and *Aspergillus*  
60 *flavus* (Almutairi 2024). In Saudi Arabia, we found only a mention about the fungus  
61 *Scedosporium apiospermum* and the species of *Fusarium*, *Verticillium*, *Purpureocillium*, and  
62 *Clavispora* that were shown to have potential bioremediation ability of heavy metal and oil-  
63 polluted material (Ameen *et al.* 2024). In the area where oil pollution is the main source of  
64 heavy metals, novel heavy metal-resistant isolates growing under oil pollution are needed. This

65 information is still lacking. In this study, novel indigenous fungal isolates were searched from  
66 oil-polluted soil.

67 To understand how well biochar and fungi can remove Zn and Cd from polluted material, we  
68 need to look at the biosorption equilibrium. Isotherm models are used to represent the  
69 distribution of metal ions between the liquid and solid phases when the system is in equilibrium  
70 (Mir en Rather, 2024; Sarangi en Rajkumar, 2024). The Langmuir, Freundlich, and Temkin  
71 isotherm models are used to investigate the equilibrium biosorption behavior of the metals  
72 (Dhaka *et al.*, 2024).

73 Our research aimed to present a sustainable bioremediation technique for heavy metal  
74 contamination in oil-polluted material. To achieve this, the following objectives were stated.  
75 First, potential heavy metal-resistant isolates were screened from contaminated soils, and the  
76 best-performing were selected for a bioremediation experiment. Second, two fungi, *Aspergillus*  
77 *niveus* and *Alternaria chlamydosporigena*, were tested to assess how well they can clean up Zn  
78 and Cd pollution together with biochar in the bioremediation experiment. Third, to understand  
79 the adsorption mechanisms of the heavy metals, kinetic and biosorption equilibrium studies  
80 were carried out.

## 81 **2. Materials and methods**

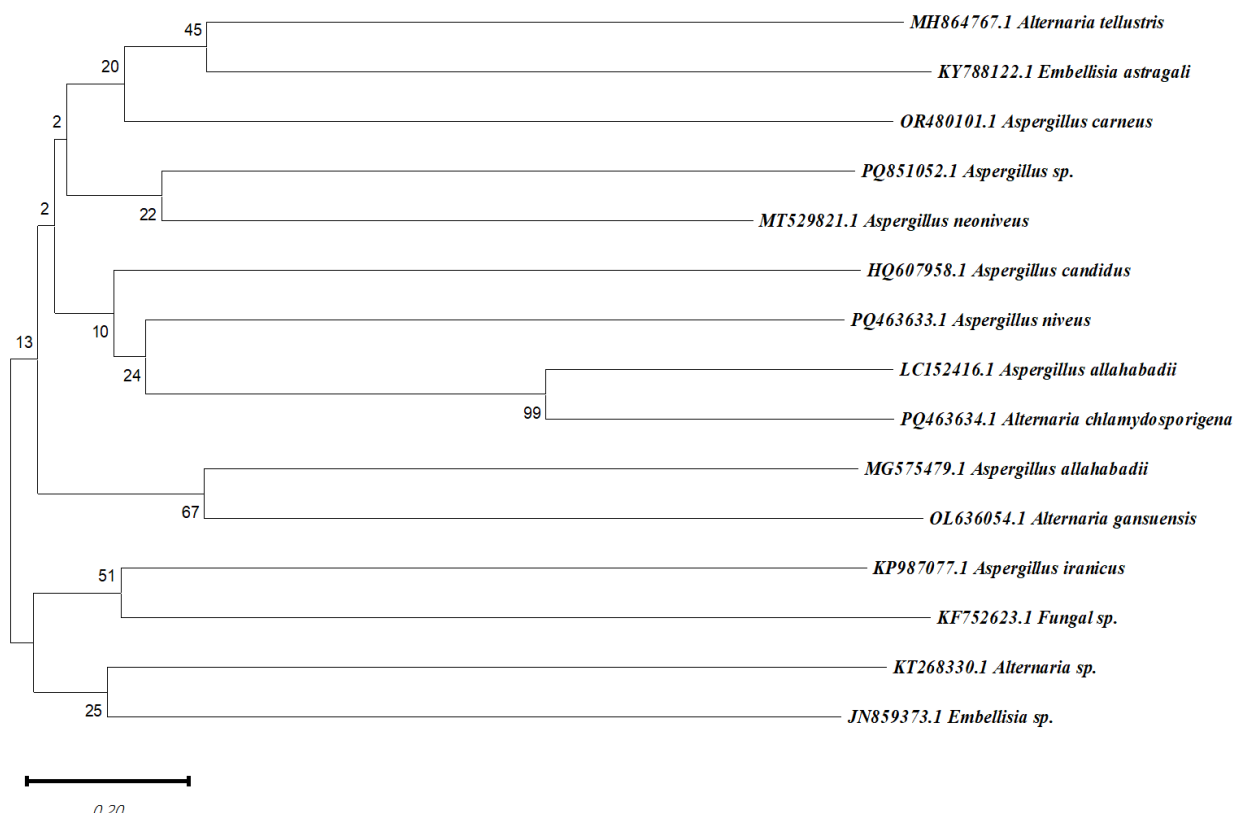
### 82 **2.1 Sample Collection and Preparation**

83 Soil samples were collected systematically from the upper 20 cm at various contaminated sites  
84 in *Al-Ahsa* and *Buqaiq*, located in Eastern Saudi Arabia (25°23'N 49°36'E). These sites are  
85 known to exhibit heavy metal contamination due to petroleum operations. Pre-sterilized  
86 stainless-steel augers were utilized to collect composite samples according to a randomized  
87 sampling grid. The samples were homogenized and promptly stored in sterile polythene bags.  
88 Samples were kept at 4°C during transport to the laboratory, utilizing insulated iceboxes to  
89 ensure microbial longevity, along with avoiding chemical transformation.

### 90 **2.2 Fungal Isolation and Identification**

91 Filamentous fungi were extracted from the soil samples using serial dilution (from  $10^{-1}$  to  $10^{-7}$ )  
92 in sterile phosphate-buffered saline (pH 7.2). For the first step, 1 gram of mixed soil was placed  
93 into 10 milliliters of clean distilled water and stirred at 220 rpm for 20 min. The suspension  
94 was permitted to sediment for 30 minutes at room temperature (Asomadu *et al.*, 2024). Samples  
95 of 100  $\mu$ L were spread out in three copies on Potato Dextrose Agar (*PDA*, *HiMedia*) with 50  
96 mg/L added.

97 Fungal colonies were selected according to their morphological characteristics and  
 98 subsequently subcultured onto fresh PDA plates using quadrant streaking. Pure isolates were  
 99 stored on PDA slants at 4°C for short-term preservation and in 20% glycerol at -80°C for long-  
 100 term storage. Chloramphenicol was added to inhibit bacterial growth. Plates were incubated at  
 101 28±1°C for 5 to 7 days (C. Wang *et al.*, 2024). Two isolates were selected based on their superior  
 102 growth performance in heavy metal-amended potato dextrose broth (200 mg/L Zn or Cd).  
 103 Genomic DNA was isolated from fresh mycelia using the CTAB technique, followed by PCR  
 104 amplification of the internal transcribed spacer (ITS) region employing the universal primers  
 105 ITS1 (5'-TCCGTAGGTGAAACCTGCGG-3') and ITS4 (5'-TCCTCCGCTTATTGATATGC-3')  
 106 (Ali *et al.*, 2024). The amplified products were sequenced in both directions, and the resulting  
 107 sequences were submitted to GenBank with accession numbers *PQ463633* and *PQ463634*,  
 108 respectively. Phylogenetic analysis was conducted with MEGA X software by matching the  
 109 ITS sequences with reference strains from NCBI. The maximum likelihood tree, created using  
 110 1000 bootstrap repetitions, showed that isolate *PQ463633* is *A. niveus* (99.8% similar to strain  
 111 CBS 115.57) and isolate *PQ463634* is *A. chlamydosporigena* (99.6% similar to strain CBS  
 112 116148) (Figure 1).



113  
 114

**Figure 1.** Phylogenetic tree of the fungal taxa obtained using the Neighbor-Joining method using the MEGA11 software

115 *2.2.1 Metal tolerance of fungi*

116 Following accepted procedures with adaptations, the heavy metal tolerance of *A. niveus*  
117 (*PQ4636*) and *A. chlamydosporigena* (*PQ4636*) was assessed by dissolving analytical-grade  
118  $\text{CdCl}_2 \cdot \text{H}_2\text{O}$  (Merck, 99.9%) and  $\text{ZnSO}_4 \cdot 7\text{H}_2\text{O}$  (Sigma-Aldrich,  $\geq 99\%$ ) in ultrapure water  
119 (Milli-Q, 18.2 M $\Omega$ %), followed by serial dilution in sterile 0.1 M phosphate buffer (pH 6.5)  
120 (Amin, Nazir en Rather, 2024). Test concentrations ranged from 10–80 ppm. Five-mm  
121 mycelial plugs taken from the actively developing margins of the 7-day-old PDA cultures were  
122 inoculated onto metal-amended PDA plates ( $n=3$  per concentration) together with metal-free  
123 controls for every isolate. For 168 hours, the plates were incubated at  $25 \pm 1^\circ\text{C}$  and 60 $\pm 5\%$   
124 relative humidity. Digital calipers (Mitutoyo,  $\pm 0.01$  mm precision) and the tolerance index (Ti)  
125 were used daily along two perpendicular axes to measure colony diameters;  $\text{Ti} = (\text{R}_1/\text{R}_0) \times 100$   
126 where  $\text{R}_1$  is the mean radial growth in the metal-amended medium and  $\text{R}_0$  is the mean radial  
127 growth in the control.

128 **2.3 Bioremediation experiment**

129 Controlled liquid culture experiments were carried out. To acquire actively proliferating  
130 mycelia, fungal isolates were initially cultivated on potato dextrose agar (PDA) plates for 7  
131 days at  $25 \pm 2^\circ\text{C}$ . The experiments were carried out in 250 mL Erlenmeyer flasks that contained  
132 100 mL of potato dextrose broth (PDB) as three replicates. The flasks were supplemented with  
133 filter-sterilized aqueous solutions of  $\text{ZnSO}_4 \cdot 7\text{H}_2\text{O}$  and  $\text{CdCl}_2 \cdot \text{H}_2\text{O}$  so that the final metal  
134 concentrations were 10, 20, 40, 60, and 80 mg/L. Biochar derived from rice husk (pH 8.2,  
135 surface area 230 m $^2$ /g) was obtained from a certified agricultural supplier. Biochar was  
136 sterilized through autoclaving and 1.0 g was added to the flasks aseptically. Three 5-mm  
137 mycelial discs from the 7-day-old cultures were aseptically introduced into the flasks. The  
138 cultures were maintained at  $25 \pm 1^\circ\text{C}$  with constant agitation (150 rpm) for 7 days. After the  
139 incubation, the fungal biomass and biochar were separated via vacuum filtration using a 0.45  
140  $\mu\text{m}$  cellulose membrane, and the filtrate was preserved for residual metal analysis. The fungal  
141 biomass was dried in the oven at 60 $^\circ\text{C}$  until a constant weight was achieved. The filtrate was  
142 acidified with 2%  $\text{HNO}_3$  and analyzed using flame atomic absorption spectrophotometry (AAS;  
143 *PerkinElmer PinAAcle 900T*) with detection limits of 0.01 ppm for both metals. Metal removal  
144 % was calculated. The treatments were as follows. PDB without amendments (Control), fungal  
145 inoculation with either of the two isolates, and fungal isolation with biochar.

146 **2.4 Fourier transform infrared spectroscopy (FTIR) analyses**

147 The functional groups of the fungal biomass were analyzed using a Fourier transform infrared  
148 spectrometer (*Agilent system Cary 630 FTIR model*). To evaluate the transmittance spectra  
149 recorded between 3000-400  $\text{cm}^{-1}$ , pressed potassium bromide (KBr) pellets were used as  
150 depicted in **Figure 2**.

151 **2.5 Kinetic studies and Adsorption isotherm studies.**

152 Lagergren linear pseudo-first-order rate equation found was;

$$153 \quad \text{Log}(q_e - q_t) = \text{log} q_e - \frac{K_1 t}{2.303} \quad (i)$$

154 In this context, 'qe' (mg/g) represents the equilibrium adsorption of metal ions, while 'qt' (mg/g)  
155 denotes the adsorption at a specific time 't' (min). The rate constant for the pseudo-first-order  
156 biosorption process is represented as  $K_1$  (min $^{-1}$ ). The results for ' $K_1$ ' and 'qe' are presented in **Figure 3**  
157 displayed on a graph of  $\text{log}(q_e - q_t)$  versus time (t) in minutes.

158 This formulation is utilised to denote the pseudo-second-order model that has been developed.

$$159 \quad \frac{t}{q_t} = \frac{1}{(K_2 q_e 2)} + \frac{t}{q_e} \quad (ii)$$

160  $K_2$  represents the pseudo-second-order equilibrium rate constant measured in g/mg min, while 'qe'  
161 denotes the quantity of biosorption at equilibrium.

162

163 The Langmuir hypothesis posits that sorption takes place at distinct, uniform sites throughout  
164 the sorbent material. It is also feasible to articulate non-linear forms of this paradigm.

$$165 \quad q_e = \frac{q_m K_l C_e}{1 + K_l C_e} \quad (iii)$$

166 In this context, 'qm' denotes the monolayer sorption efficiency of the material (mg/g), while 'Ce'  
167 indicates the equilibrium metal ion concentration in the solution (mg/L). The term 'KL' refers to the  
168 Langmuir adsorption constant (mg/L), which is associated with the free energy of sorption, and 'qe'  
169 represents the equilibrium metal ion content of the sorbent (mg/g).

170 The Freundlich model suggests that the sorption surface exhibits a variety of characteristics.

171 The Freundlich model is

$$172 \quad q_e = K_f C_e^{1/n} \quad (iv)$$

173 In this context, 'Kf' represents a constant that characterizes the biosorption capacity, while '1/n' serves  
174 as an observational variable. This outlines the degree of biosorption, which varies based on the  
175 differences in the material used. The values of 'Kf' and '1/n' were determined through nonlinear  
176 regression analysis. (**Figure 4**) presents the graphs of the non-linear Freundlich isotherm. The values  
177 of '1/n' ranging from '0' to '1' suggest that the biosorption was effective under the examined conditions

178 **2.6 Statistical Analysis**

179 One-way ANOVAs were carried out using SPSS version 20. Mann Whitney test was used to  
180 compare the concentration treatments to the control. The p-value less than 0.05 was assessed  
181 as a statistically significant difference.

182 **3. Results**

183 **3.1. Fungal heavy metal tolerance**

184 *Alternaria chlamydosporigena* showed that its growth was affected by the amount of both  
185 metals, with Zn causing a noticeable reduction in its growth at all tested levels (10–80 ppm; p  
186 = 0.050) (**Table 1**). The tolerance indices (Ti) for Zn dropped steadily from 80.9% at 10 ppm  
187 to 28.6% at 80 ppm, showing a 64.6% decrease in growth ability. Similarly, exposure to Cd  
188 caused a growth reduction, but Ti was higher (82.1% at 10 ppm to 52.3% at 80 ppm), showing  
189 that the fungus was more resistant to Cd. One-way ANOVA established the inverse correlation  
190 between the metal content and fungal vitality. The rate of growth inhibition was much greater  
191 for Zn (slope = -0.65% per ppm) compared to Cd (slope = -0.37% per ppm).

192 **Table 1:** *A. chlamydosporigena* fungal growth and tolerance index in increasing Zn and Cd  
193 concentrations. \* refers to the significant difference to control.

194

Zn concentration, mg/L	Growth, mm	Tolerance Index
0, Control	7.68±0.07	
10	6.30±0.05	<b>82.10%*</b>
20	5.88±0.16	<b>76.6%*</b>
40	5.45±0.11	<b>70.96%*</b>
60	5.02±0.09	<b>66.23%*</b>
80	4.03±0.08	<b>52.30%*</b>
Cd concentration mg/l.		
0, control	7.68±0.07	
10	6.23±0.03	<b>80.90%*</b>
20	5.49±0.06	<b>71.50%*</b>
40	3.73±0.03	<b>48.00%*</b>
60	3.18±0.24	<b>41.60%*</b>
80	2.18±0.16	<b>28.60%*</b>

206

207 The growth of *A. niveus* was significantly lower at 10, 20, 40, 60, and 80 ppm than in  
208 the control. The tolerance indices for concentrations of 10, 20, 40, 60, and 80 ppm were

209 87.50%, 68.80%, 48.90%, 41.30%, and 39.80%, respectively. The growth was significantly  
210 reduced at 10, 20, 40, 60, and 80 ppm Cd in comparison to the control. In the Cd concentrations  
211 40 mg/L and higher, no growth was observed. The tolerance indices measured at 10, 20, 40,  
212 60, and 80 ppm were 48.20%, 27.50%, 0%, 0%, and 0%, respectively (**Table 2**).

213 **Table 2:** *A. niveus* fungal growth and tolerance index in increasing Zn and Cd concentrations.  
214 \* refers to the significant difference from control.

215  
216

Zn concentration, mg/L	Sample	Tolerance Index
0, Control	6.55±0.05	
10	5.72±0.03	<b>87.50%*</b>
20	4.50±0.01	<b>68.80%*</b>
40	3.20±0.05	<b>48.90%*</b>
60	2.72±0.03	<b>41.30%*</b>
80	2.55±0.05	<b>39.80%*</b>

Cd concentration mg/l.		
0, Control	6.55±0.05	--
20	1.77±0.25	<b>27.50%*</b>
40	0	<b>0*</b>
60	0	<b>0*</b>
80	0	<b>0*</b>

217  
218

### 219 **3.2 Heavy metal removal by fungi and biochar**

220 *A. chlamydosporigena* reduced all experimental Zn concentrations significantly. The combined  
221 use of *A. chlamydosporigena* and biochar reduced the metals more than the fungus alone. The  
222 reduction was 35–55% ( $p = 0.050$ ), being highest at the medium concentrations (40–60 ppm).  
223 Significant differences between the treatments ( $F = 8.34$ ,  $p < 0.05$ ) were observed for all  
224 concentrations.

225 **Table 3:** Concentrations of Zinc (Zn) and Cadmium (Cd) in treatments involving *Aspergillus*  
226 *chlamydosporigena* (fungi) and a combination of fungi with biochar under varying Zn  
227 concentrations in the culturing medium. \* refers to the significant difference from control.

228  
229  
230  
231

Zn concentration, mg/L		
Culturing medium	Fungi	Fungi+biochar
0, Control	0.00±0.00	<b>0.00±0.00</b>
10	4.90±0.26	<b>2.03±0.25*</b>
20	9.37±0.57	<b>5.23±0.42*</b>
40	17.20±0.89	<b>10.08±1.07*</b>
60	24.41±0.71	<b>16.40±0.60*</b>
80	38.63±1.18	<b>22.63±0.65*</b>
Cd concentration mg/l.		
Culturing medium	Fungi	Fungi+biochar
0, control	0.00±0.00	<b>0.00±0.00</b>
10	4.40±0.78	<b>2.03±0.25*</b>
20	13.34±0.67	<b>5.23±0.42*</b>
40	24.54±0.67	<b>10.08±1.07*</b>
60	37.87±1.13	<b>16.40±0.60*</b>
80	53.55±0.45	<b>22.63±0.65*</b>

232

233

234 The adsorption of zinc and cadmium with *A. niveus* was greatly improved by the  
 235 addition of biochar at all doses. For zinc, the combination of fungi and biochar consistently  
 236 showed lower leftover amounts compared to fungi alone, being statistically significant at all  
 237 tested levels ( $p = 0.050$  at 10/40/60/80 ppm;  $p = 0.046$  at 20 ppm) (Table 3). For cadmium, a  
 238 similar trend was observed, where the combination of fungi and biochar significantly lowered  
 239 soluble Cd levels ( $p = 0.050$ ) at all concentrations compared to the treatment with only fungi.

240 **Table 4:** Zinc (Zn) and Cadmium (Cd) concentrations in treatments with *A. niveus* (fungi) and fungi  
 241 combined with biochar under increasing Zn concentrations in the culturing medium. \* refers to the  
 242 significant difference from control.

243

Zn concentration, mg/L		
Zn concentration mg/l	Fungi+Zn	Fungi+Zn+biochar
0, Control	0.00±0.00	<b>0.00±0.00</b>
10	1.85±0.44	<b>0.18±0.07*</b>
20	3.93±0.96	<b>0.42±0.03*</b>
40	8.53±0.61	<b>5.10±0.6*</b>
60	24.08±1.03	<b>8.77±0.25*</b>
80	23.37±3.73	<b>12.07±0.21*</b>
Cd concentration mg/l		
Cd concentration mg/l	Fungi+Cd	Fungi+Cd+biochar
0, Control	0.00±0.00	<b>0.00±0.00</b>
10	1.85±0.44	<b>0.18±0.07*</b>
20	3.93±0.96	<b>0.42±0.03*</b>
40	8.53±0.61	<b>5.10±0.6*</b>

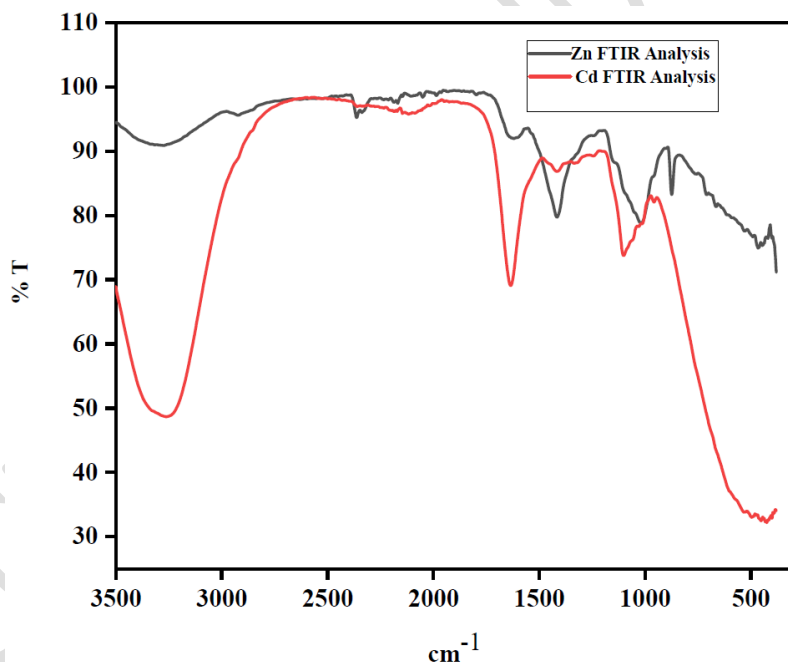
60	24.08±1.03	8.77±0.25*
80	23.37±3.73	12.07±0.21*

244

245 **3.3 FTIR Analysis**

246 The biggest changes were seen in the range of 1800-1200  $\text{cm}^{-1}$ , where carboxylate groups  
 247 ( $\text{COO}^-$ ) shifted down in frequency by 1822  $\text{cm}^{-1}$  during their symmetric stretching vibrations  
 248 (from 1420 to 1398  $\text{cm}^{-1}$  for Zn and from 1420 to 1402  $\text{cm}^{-1}$  for Cd) in (Figure 2). The  
 249 decrease (34%) in the peak intensity of carbonyl ( $\text{C=O}$ ) at 1720  $\text{cm}^{-1}$  was observed. Protein  
 250 components showed 12-15% widening in the amide I ( $1650 \text{ cm}^{-1}$ ) and amide II ( $1540 \text{ cm}^{-1}$ )  
 251 bands. Shoulders appeared around 1580-1560  $\text{cm}^{-1}$ , which is indicative of metal-nitrogen  
 252 bonding. Stronger phosphoryl ( $\text{P=O}$ ) signals at 1220  $\text{cm}^{-1}$  and stronger vibrations from  
 253 polysaccharides at 1050  $\text{cm}^{-1}$  were observed. Zn-O vibration at 620  $\text{cm}^{-1}$  and Cd-S at 550  $\text{cm}^{-1}$   
 254 were observed in Zn and Cd treatments, respectively.

255



256

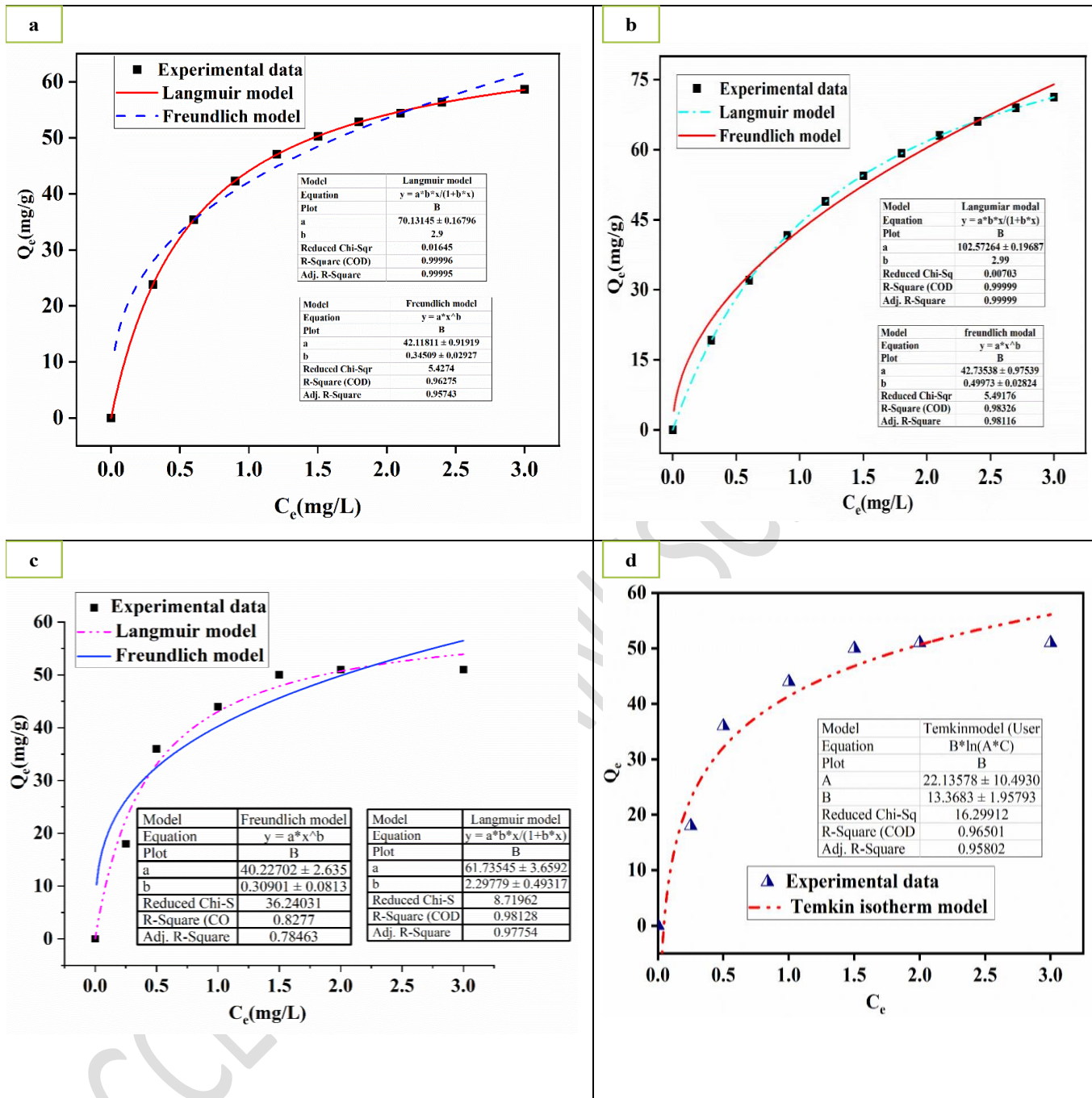
257

258 **Figure 2.** FTIR Study analysis259 **3.4 Kinetic Studies**

260 The pseudo-first-order model assumes that each metal ion attaches to one specific spot on the

261 **Figure 3.** Kinetic study analysis. (a) pseudo first order, (b) pseudo second order, (c) Intra particular diffusion,  
 262 (d)Elovich model

263 order reaction, is represented by the linear formulation provided above.



264

### 265 3.5 Biosorption Isotherm Models

266 The Langmuir model demonstrated the greatest fit to the experimental data ( $R^2 > 0.98$ ),  
 267 followed by the Freundlich model ( $R^2 = 0.92-0.95$ ) and the Temkin model ( $R^2 = 0.85-0.89$ ).  
 268 The Langmuir analysis showed the maximum adsorption capacities ( $q_{\text{mas}}$ ) for Zn (II) and for  
 269 Cd (II). Furthermore, the affinity constants ( $K_l$ ) were high. Dimensionless separation factors  
 270 ( $R_l$ ) ranged from 0.02 to 0.35. The Freundlich model exhibited a somewhat weaker correlation,  
 271 with its heterogeneity value ( $1/n = 0.42-0.58 < 1$ ). According to the Temkin model, moderate  
 272 adsorption heats were observed ( $b_2 = 120-180 \text{ J/mol}$ ).

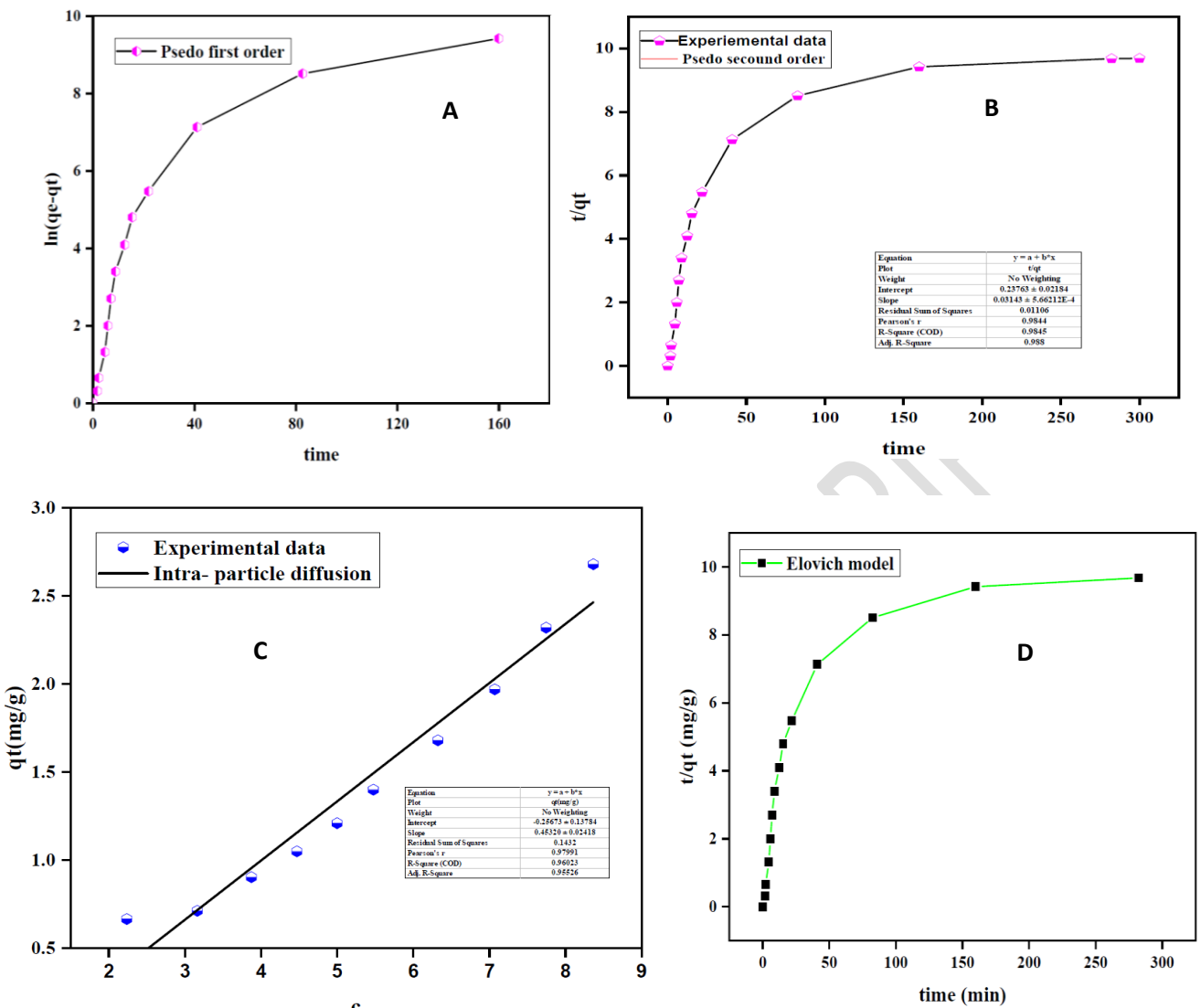


Fig. 4. Biosorption study analysis. Langmuir: Freundlich: Temkin models

273

274

275

276

277

278

### 279 3.6 Discussion

280 The two native fungal isolates were efficient in reducing Zn and Cd concentrations. However,  
 281 the leftover metal concentrations were still too high when either of the fungi was incubated.  
 282 This showed that the natural ability of the fungi to remove metals was limited. It is known that  
 283 certain species can adsorb heavy metals. These fungi have often been isolated from heavy  
 284 metal-polluted sites such as *A. terreus* and *A. hiratsukae* in Oman (Palanivel, Pracejus en Novo,

285 2023) Moreover, other pollution seems to induce the stress-resistance of fungi. Several  
286 *Aspergillus* species have shown to adsorb Cr, Zn, Cu, Cd, and Ni efficiently (Vašinková,  
287 Dlabaja en Kučová, 2021; Narolkar, Jain en Mishra, 2022). The heavy metal-resistant strain of  
288 *A. flavus* was isolated from an oil-polluted soil (Al-Dhabaan, 2022). It has also been found that  
289 the combined pollution of heavy metals and oil generates resistant fungal strains. The efficiency  
290 of these fungi to adsorb pollutants is due to the secreted extracellular enzymes and other  
291 metabolites (Li, Liu en Gadd, 2020).

292 The efficiency of metal reduction was increased remarkably when rice husk biochar was added  
293 together with the fungi. The system exhibited its highest efficiency at the concentration of 40  
294 ppm, removing 86.5% Zn and 89.2% Cd. We interpret that *A. chlamydosporigena* alone is not  
295 enough efficient to reduce the metal concentrations, but together with biochar, the remediation  
296 process is highly efficient. This is due to the three benefits that biochar provides: (i)  
297 supplementary binding sites, (ii) toxicity buffering for fungal cells, and (iii) pH stabilization  
298 with the final pH of 6.8 (Chen *et al.*, 2022).

299 Based on the consistent patterns observed, it can be inferred that biochar contributes  
300 through various mechanisms (Gorovtsov *et al.*, 2020). Firstly, it offers additional adsorption  
301 sites through its porous matrix. Secondly, it alters the metal speciation by elevating the pH  
302 level. Lastly, biochar has the potential to protect fungal biomass from the harmful effects of  
303 metals. In our study, the ability of biochar to improve fungal cleanup was shown to be effective  
304 at all concentrations, with the most effective at 20 ppm Zn. Specifically, in moderately Zn-  
305 contaminated systems (20–60 ppm), biochar increased metal immobilization by 38–52%  
306 compared to fungal treatment alone. Our findings established that rice husk biochar was an  
307 efficient amendment for *A. niveus*-based bioremediation.

308 FTIR provided molecular-level evidence of the mechanisms that underlie heavy metal  
309 biosorption in the fungal-biochar systems (Racić *et al.*, 2023; Nandasana, Thongmee en Ghosh,  
310 2024). After comparing the spectral profiles of biomass exposed to metals and those that were  
311 not, it was found that important functional groups changed. Carboxylate (COO<sup>-</sup>) and carbonyl  
312 (C=O) groups shifted down in frequency. These alterations provide further evidence that  
313 carboxyl groups play an essential part in the coordination of metals through intramolecular  
314 interactions. Protein components showed important changes in structure, shown by a 12-15%  
315 widening of the bands of amides. Moreover, metal-nitrogen bonding was observed. Spectral  
316 fingerprints that were unique to the fungal-biochar composites were observed previously (Zhao

317 *et al.*, 2024). These unique signals included stronger phosphoryl and polysaccharides signals  
318 indicating the creation of ternary complexes between the fungal cell walls, metals, and biochar  
319 surfaces. The metal-specific signatures were particularly noteworthy. The exposure to zinc  
320 resulted in the generation of a distinct Zn-O vibration at 620 cm<sup>-1</sup>. The treatment with cadmium  
321 resulted in the production of a Cd-S stretching band at 550 cm<sup>-1</sup>. This suggests that Zn has a  
322 preference for oxygen-dominated coordination, whereas Cd was involved in sulfur  
323 participation (Nandasana, Thongmee, and Ghosh, 2024). The spectroscopic evidence as a  
324 whole demonstrates that biochar improves the process of metal sequestration in fungi by the  
325 following mechanisms: (i) protecting essential fungal binding sites from the toxicity of metals;  
326 (ii) introducing additional oxygen-containing functional groups; and (iii) facilitating the  
327 formation of stable ternary complexes. These molecular-scale interactions provide an  
328 explanation for the reported 35-55% boost in metal removal efficiency that occurs when  
329 biochar amendment is combined with fungal therapy.

330 Kinetic studies are crucial for clarifying the reaction mechanisms and rates of solute absorption  
331 in biosorption processes. This is especially true in bioremediation systems that are aimed to  
332 reduce heavy metals such as Zn and Cd (Karnwal, 2024; Mir en Rather, 2024). The findings  
333 from these studies provide important information about how metal ions interact with  
334 biosorbents like biochar or fungal biomass at the surface where solid and liquid meet. These  
335 dynamics have a direct impact on the effectiveness of contaminant removal. In the framework  
336 of this investigation, pseudo-first-order and pseudo-second-order models were utilized to  
337 assess the biosorption kinetics of Zn and Cd by biochar and fungi (Xie, 2024). The pseudo-  
338 first-order model assumes that each metal ion attaches to one specific spot on the surface of the  
339 biosorbent (Al-Homaidan *et al.*, 2018). On the other hand, the pseudo-second-order model  
340 proposes the existence of chemisorption mechanisms, in which adsorption is characterized by  
341 the presence of shared active sites or contacts that are influenced by electrostatic forces,  
342 chemical bonding, or ion exchanges. The pseudo-second-order model is typically more suitable  
343 for estimating bioremediation kinetics. This advantage is due to the fact that heavy metal  
344 biosorption frequently follows chemisorption, which is a process of the second order (P. Wang  
345 *et al.*, 2024).

346 Comprehending the kinetics of metal biosorption is crucial for enhancing bioremediation  
347 strategies in oil-contaminated environments, as it offers vital information regarding the  
348 efficiency, mechanism, and scalability of the process. Kinetic parameters, including  $K_1$ ,  $K_2$ , and  
349  $q_e$ , are essential for quantifying the rate and extent of metal removal. This quantification

350 facilitates the design of efficient large-scale remediation systems. A high correlation coefficient  
351 ( $R^2$ ) for the pseudo-second-order model, aligning with findings from analogous studies on Cu,  
352 suggests that chemisorption is the primary mechanism for the uptake of Zn and Cd by biochar  
353 and fungi. The involvement of functional groups, such as carboxyl and hydroxyl, found in  
354 fungal cell walls and biochar surfaces supports this process by facilitating metal binding  
355 through chemical interactions. Kinetic data also establish the necessary residence time for both  
356 batch and continuous-flow systems, facilitating effective and efficient implementation in  
357 oilfield remediation.

358 Isotherm models help us understand how the biosorbents attract and hold onto metals,  
359 their surface features, and how much metal they can absorb at most (Mir en Rather, 2024;  
360 Sarangi en Rajkumar, 2024). The results showed that monolayer adsorption was the  
361 predominant mode of action in the biosorption process. The Langmuir analysis showed the  
362 maximum adsorption capacities. Furthermore, the affinity constants were high, which indicated  
363 that there were significant interactions between the metal and the biosorbent. Further  
364 confirmation of the favorable adsorption conditions was provided by dimensionless separation  
365 factors. Despite the fact that the Freundlich model exhibited a somewhat weaker correlation,  
366 its heterogeneity value indicated a certain degree of multilayer adsorption and surface  
367 heterogeneity. This is most likely due to the porous structure of biochar and the different  
368 functional groups that are present on fungal biomass (Medina-Armijo *et al.*, 2024). According  
369 to the Temkin model, moderate adsorption heats were observed, which suggests that  
370 electrostatic interactions play a role in the binding mechanism.

371 These data collectively show that chemisorption is the major adsorption mechanism  
372 and that it occurs through mechanisms such as ion exchange and surface complexation.  
373 However, it is important to note that there is some variation in the binding site energies because  
374 of these discoveries. This validates the creation of a homogeneous monolayer of metal ions on  
375 the biosorbent surfaces, which is essential for forecasting and optimizing remediation  
376 effectiveness in field applications. The superior fit of the Langmuir model has important  
377 practical consequences since it confirms the formation of this monolayer. This biochar-fungal  
378 system has a strong potential for effective heavy metal removal from contaminated oil sites, as  
379 demonstrated by the high  $q_{\text{mas}}$  values that were obtained. Additionally, the secondary Freundlich  
380 characteristics indicate that there are opportunities for further enhancement through  
381 modification of surface properties in order to take advantage of multilayer adsorption. These  
382 findings highlight the significance of isotherm analysis for gaining knowledge and improving

383 contaminant removal processes, offering substantial insights that can be utilized in developing  
384 effective bioremediation strategies (Meena *et al.*, 2018). A homogenous, monolayer-driven  
385 biosorption of the metals is highlighted by the best-fit state of the Langmuir isotherm. On the  
386 other hand, the Freundlich and Temkin models offer supplementary insights into surface  
387 heterogeneity and interaction energies.

388 It has been shown that fungi and biochar have synergistic effects in the remediation of  
389 different pollutants. The combination was efficient to remediate the combined pollution of  
390 organic pollutants and heavy metals (Xia *et al.*, 2025). Elsewhere, biochar and bacteria were  
391 shown to be efficient in the remediation of oil-contaminated soil (Li *et al.*, 2025). Moreover,  
392 biochar and fungi were efficient in remediating various pollutants (Pai *et al.*, 2024). Our results  
393 support the previous findings that biochar-fungal systems are effective for the removal of heavy  
394 metals, and thus, we can provide recommendations for the development of future strategies.

395 When used with fungal biomass, biochar's large surface area ( $230\text{ m}^2/\text{g}$ ) and ability to exchange  
396 cations (24.5 cmol+/kg) led to more metal being absorbed. This was accomplished through  
397 both physical binding and chemical interactions (Awasthi *et al.*, 2021). In subsequent research,  
398 it is recommended to explore the long-term metal stability and field-scale performance of this  
399 consortium consisting of biochar and plants.

### 400 **3.7 Conclusion and Recommendations**

401 The findings of this study show that the local fungi *A. niveus* (PQ463633) and *A.*  
402 *chlamydosporigena* (PQ463634) could effectively clean up soils contaminated with zinc and  
403 cadmium in eastern Saudi Arabia. Adsorption isotherm analysis confirmed Langmuir  
404 monolayer adsorption as the major mechanism, with the Freundlich and Temkin models  
405 indicating additional heterogeneous binding interactions. The isolates displayed remarkable  
406 metal resistance and biosorption capacity. Kinetic studies showed that the metals were taken  
407 up quickly, and Fourier transform infrared spectroscopy revealed that the metals were actively  
408 bound through interactions with functional groups. A promising combined approach for real-  
409 world use is shown by the improved cleanup effectiveness gained by adding biochar. The  
410 selected fungal strains were able to remove significant amounts of heavy metals by  
411 simultaneously utilizing a combination of biosorption and bioaccumulation mechanisms, and  
412 the addition of biochar resulted in a considerable improvement in the efficacy of the  
413 remediation process by increasing the immobilization of metals. The balance of the data was

414 best explained by the Langmuir isotherm model, showing that chemisorption was the main  
415 process at work.

416 Furthermore, the genetic and proteomic investigations may elucidate the molecular  
417 resistance mechanisms of these fungal species. The study's results establish a foundation for  
418 environmentally friendly, nature-based remediation technologies that may supplant energy-  
419 intensive methods in oil-contaminated regions. Subsequent research should investigate the  
420 scalability of this strategy and evaluate the regulatory frameworks necessary for its  
421 implementation.

422 **Author Contributions:** The final draft of the work has been reviewed and approved by all au-  
423 thors.

424 **Conflict of interest:** The authors declare that they have no conflicts of interest.

425 **Acknowledgments**

426 The authors extend their appreciation to the ongoing research funding program (ORF-2025-  
427 364), King Saud University, Riyadh, Saudi Arabia.

428

429 **References**

430 Al-Dhabaan, F.A. (2022) “Characterization of Cadmium and Lead Heavy Metals Resistant  
431 Fungal Isolates from Ghawar oil field, Saudi Arabia”, *Biosciences Biotechnology Research  
432 Asia*, 19(3), bll 625–633. Available at: <https://doi.org/10.13005/bbra/3015>.

433 Al-Homaidan, A.A. *et al.* (2018) “Potential use of green algae as a biosorbent for hexavalent  
434 chromium removal from aqueous solutions”, *Saudi Journal of Biological Sciences*, 25(8), bll  
435 1733–1738. Available at: <https://doi.org/10.1016/j.sjbs.2018.07.011>.

436 Ali, S.A. *et al.* (2024) “the Endophytic Fungus Epicoccum Nigrum: Isolation, Molecular  
437 Identification and Study Its Antifungal Activity Against Phytopathogenic Fungus Fusarium  
438 Solani”, *Journal of Microbiology, Biotechnology and Food Sciences*, 13(5), bll 10093– 10093.  
439 Available at: <https://doi.org/10.55251/jmbfs.10093>.

440 Almutairi, H. (2024). Microbial communities in petroleum refinery effluents and their complex  
441 functions. *Saudi Journal of Biological Sciences*. <https://doi.org/10.1016/j.sjbs.2024.104008>.

442 Ameen, F., Alsarraf, M., Abalkhail, T. Stephenson, S. (2024). Evaluation of resistance patterns  
443 and bioremoval efficiency of hydrocarbons and heavy metals by the mycobiome of petroleum  
444 refining wastewater in Jazan with assessment of molecular typing and cytotoxicity of  
445 *Scedosporium apiospermum* JAZ-20. *Heliyon*. <https://doi.org/10.1016/j.heliyon.2024.e32954>.

446 Amin, I., Nazir, R. en Rather, M.A. (2024) “Evaluation of multi-heavy metal tolerance traits  
447 of soil-borne fungi for simultaneous removal of hazardous metals”, *World Journal of  
448 Microbiology and Biotechnology*, 40(6), bl 175. Available at: <https://doi.org/10.1007/s11274-024-03987-z>.

450 Asomadu, R.O. *et al.* (2024) “Exploring the antioxidant potential of endophytic fungi: a review  
451 on methods for extraction and quantification of total antioxidant capacity (TAC)”, *3 Biotech*,  
452 bl 127. Available at: <https://doi.org/10.1007/s13205-024-03970-3>.

453 Awasthi, S.K. *et al.* (2021) “Sequential presence of heavy metal resistant fungal communities  
454 influenced by biochar amendment in the poultry manure composting process”, *Journal of  
455 Cleaner Production*, 291, bl 125947. Available at:  
456 <https://doi.org/10.1016/j.jclepro.2021.125947>.

457 Chen, L. *et al.* (2022) “Removal of heavy-metal pollutants by white rot fungi: Mechanisms,  
458 achievements, and perspectives”, *Journal of Cleaner Production*, 354, bl 131681. Available at:  
459 <https://doi.org/10.1016/j.jclepro.2022.131681>.

460 Dhaka, R. *et al.* (2024) “Biosorption of lead (II) ions by lead-tolerant fungal biomass isolated  
461 from electroplating industry effluent”, *International Journal of Environmental Science and  
462 Technology*, 22(5), bll 2955–2966. Available at: <https://doi.org/10.1007/s13762-024-05796-1>.

463 Dinakarkumar, Y. *et al.* (2024) “Fungal bioremediation: An overview of the mechanisms,  
464 applications and future perspectives”, *Environmental Chemistry and Ecotoxicology*, 6, bll 293–  
465 302. Available at: <https://doi.org/10.1016/j.enceco.2024.07.002>.

466 Falih, K.T. *et al.* (2024) “Assessment of petroleum contamination in soil, water, and  
467 atmosphere: a comprehensive review”, *International Journal of Environmental Science and  
468 Technology*, 21(13), bll 8803–8832. Available at: <https://doi.org/10.1007/s13762-024-05622-8>.

470 Gorovtsov, A. V. *et al.* (2020) “The mechanisms of biochar interactions with microorganisms

471 in soil”, *Environmental Geochemistry and Health*, 42(8), bl 2495–2518. Available at:  
472 <https://doi.org/10.1007/s10653-019-00412-5>.

473 Hou, D. *et al.* (2025) “Global soil pollution by toxic metals threatens agriculture and human  
474 health”, *Science (New York, N.Y.)*, 388(6744), bl 316–321. Available at:  
475 <https://doi.org/10.1126/science.adr5214>.

476 Karnwal, A. (2024) “Unveiling the promise of biosorption for heavy metal removal from water  
477 sources”, *Desalination and Water Treatment*, 319, bl 100523. Available at:  
478 <https://doi.org/10.1016/j.dwt.2024.100523>.

479 Li, Q., Liu, J. en Gadd, G.M. (2020) “Fungal bioremediation of soil co-contaminated with  
480 petroleum hydrocarbons and toxic metals”, *Applied Microbiology and Biotechnology*, 104(21),  
481 bl 8999–9008. Available at: <https://doi.org/10.1007/s00253-020-10854-y>.

482 Li, X. *et al.* (2025) “Synergistic biochar-microbe interactions enhance petroleum contaminant  
483 removal and microbial community succession”, *Environmental Technology and Innovation*,  
484 40, bl 104465. Available at: <https://doi.org/10.1016/j.eti.2025.104465>.

485 Liu, X. *et al.* (2024) “Frontiers in Environmental Cleanup: Recent Advances in Remediation  
486 of Emerging Pollutants from Soil and Water”, *Journal of Hazardous Materials Advances*, bl  
487 100461. Available at: <https://linkinghub.elsevier.com/retrieve/pii/S2772416624000627>.

488 Medina-Armijo, C. *et al.* (2024) “The Metallotolerance and Biosorption of As(V) and Cr(VI)  
489 by Black Fungi”, *Journal of Fungi*, 10(1), bl 47. Available at:  
490 <https://doi.org/10.3390/jof10010047>.

491 Meena, R.A.A. *et al.* (2018) “Heavy metal pollution in immobile and mobile components of  
492 lentic ecosystems—a review”, *Environmental Science and Pollution Research*, 25(5), bl  
493 4134–4148. Available at: <https://doi.org/10.1007/s11356-017-0966-2>.

494 Mir, D.H. en Rather, M.A. (2024) “Kinetic and thermodynamic investigations of copper (II)  
495 biosorption by green algae Chara vulgaris obtained from the waters of Dal Lake in Srinagar  
496 (India)”, *Journal of Water Process Engineering*, 58, bl 104850. Available at:  
497 <https://doi.org/10.1016/j.jwpe.2024.104850>.

498 Nandasana, M., Thongmee, S. en Ghosh, S. (2024) “Microbial Biochar Based Sustainable  
499 Waste Management Approach”, in *Environmental Science and Engineering*. Cham: Springer  
500 International Publishing, bl 121–145. Available at: [https://doi.org/10.1007/978-3-031-62898-6\\_6](https://doi.org/10.1007/978-3-031-62898-6_6).

502 Narolkar, S., Jain, N. en Mishra, A. (2022) “Biosorption of Chromium by Fungal Strains  
503 Isolated from Industrial Effluent Contaminated Area”, *Pollution*, 8(1), bl 159–168. Available  
504 at: <https://doi.org/10.22059/POLL.2021.326818.1132>.

505 Nna, P.J., Orie, K.J. en Kalu, N.A.S. (2024) “Source Apportionment and Health Risk of Some  
506 Organic Contaminants in Water and Suspended Particulate Matter from Imo River, Nigeria”,  
507 *Journal of Applied Sciences and Environmental Management*, 28(2), bl 291–303. Available  
508 at: <https://doi.org/10.4314/jasem.v28i2.1>.

509 Pai, S. *et al.* (2024) “Synergistic interactions of fungi and biochar for various environmental  
510 applications”, in *Bioprospecting of Multi-tasking Fungi for a Sustainable Environment: Volume I*. Singapore: Springer Nature Singapore, bl 219–247. Available at:  
512 [https://doi.org/10.1007/978-981-97-4113-7\\_10](https://doi.org/10.1007/978-981-97-4113-7_10).

513 Palanivel, T.M., Pracejus, B. en Novo, L.A.B. (2023) “Bioremediation of copper using

514 indigenous fungi *Aspergillus* species isolated from an abandoned copper mine soil”,  
515 *Chemosphere*, 314, bl 137688. Available at:  
516 <https://doi.org/10.1016/j.chemosphere.2022.137688>.

517 Racić, G. *et al.* (2023) “Screening of Native *Trichoderma* Species for Nickel and Copper  
518 Bioremediation Potential Determined by FTIR and XRF”, *Microorganisms*, 11(3), bl 815.  
519 Available at: <https://doi.org/10.3390/microorganisms11030815>.

520 Sarangi, N.V. en Rajkumar, R. (2024) “Biosorption potential of *Stoechospermum marginatum*  
521 for removal of heavy metals from aqueous solution: Equilibrium, kinetic and thermodynamic  
522 study”, *Chemical Engineering Research and Design*, 203, bll 207–218. Available at:  
523 <https://doi.org/10.1016/j.cherd.2024.01.020>.

524 Vašinková, M., Dlabaja, M. en Kučová, K. (2021) “Bioaccumulation of toxic metals by fungi  
525 of the genus *Aspergillus* isolated from the contaminated area of Ostramo Lagoons”, *IOP  
526 Conference Series: Earth and Environmental Science*, 900(1), bl 12048. Available at:  
527 <https://doi.org/10.1088/1755-1315/900/1/012048>.

528 Wang, C. *et al.* (2024) “Isolation and Identification of Pear Ring Rot Fungus and Resistance  
529 Evaluation of Different Pear Varieties”, *Horticulturae*, 10(11). Available at:  
530 <https://doi.org/10.3390/horticulturae10111152>.

531 Wang, P. *et al.* (2024) “Bio-sorption capacity of cadmium and zinc by *Pseudomonas monteili*  
532 with heavy-metal resistance isolated from the compost of pig manure”, *Bioresource  
533 Technology*, 399, bl 130589. Available at: <https://doi.org/10.1016/j.biortech.2024.130589>.

534 Wang, W. *et al.* (2024) “Biochar remediates cadmium and lead contaminated soil by  
535 stimulating beneficial fungus *Aspergillus* spp.”, *Environmental Pollution*, 359, bl 124601.  
536 Available at: <https://doi.org/10.1016/j.envpol.2024.124601>.

537 Xia, Y. *et al.* (2025) “An efficient fungi-biochar-based system for advancing sustainable  
538 management of combined pollution”, *Environmental Pollution*, 367, bl 125649. Available at:  
539 <https://doi.org/10.1016/j.envpol.2025.125649>.

540 Xie, S. (2024) “Biosorption of heavy metal ions from contaminated wastewater: an eco-  
541 friendly approach”, *Green Chemistry Letters and Reviews*, 17(1), bl 2357213. Available at:  
542 <https://doi.org/10.1080/17518253.2024.2357213>.

543 Zhao, Z. *et al.* (2024) “Combined microbe-plant remediation of cadmium in saline-alkali soil  
544 assisted by fungal mycelium-derived biochar”, *Environmental Research*, 240, bl 117424.  
545 Available at: <https://doi.org/10.1016/j.envres.2023.117424>.

546